
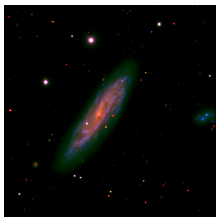
LBT & Image

"X-RAY SPECTROSCOPY OF BROMINE COMPOUNDS AND BIOMEDICAL APPLICATIONS"

SULTANA N. NAHAR

Astronomy: Anil Pradhan
Biophysics: Yi Luo, Linh Le, Sara Lim,
Physics: Enam Chowdhury
Chemistry: Russel M. Pitzer
The Ohio State University, USA
Maximiliano Montenegro
Catholic University of Chile, Chile

65th "INTERNATIONAL SYMPOSIUM ON MOLECULAR SPECTROSCOPY"
The Ohio State University, Columbus, Ohio, USA
June 21-25, 2010

Support: Large Interdisciplinary Grant - OSU, NASA APRA
Computations - Ohio Supercomputer Center (OSC), Columbus, Ohio

NANOBIO-SPECTROSCOPY

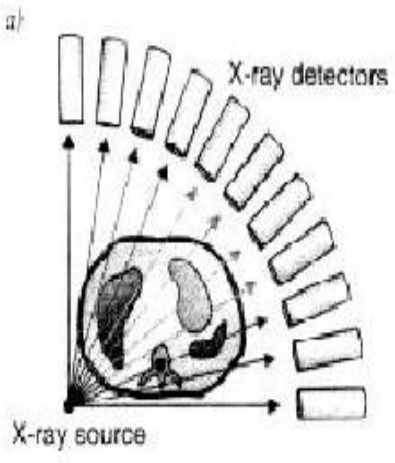

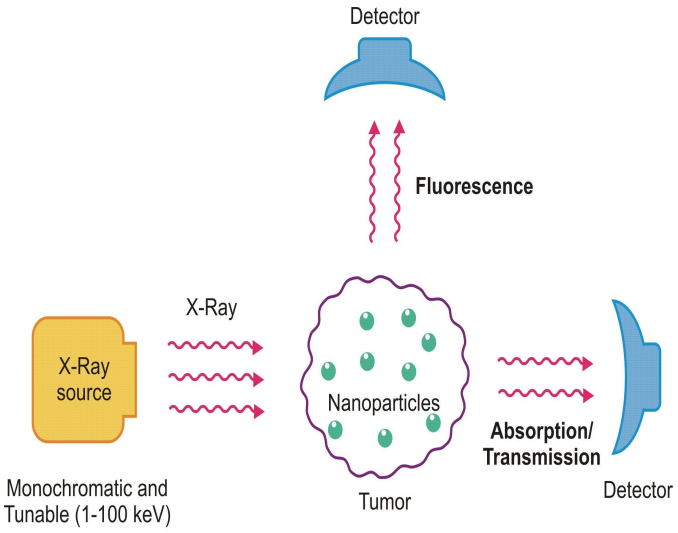

OBJECTIVE: Spectroscopy over Imaging

- Biomedical methods use intense and broadband high energy X-rays in radiation therapy and diagnostics (theranostics) to ensure sufficient tissue penetration (left Fig)
- To avoid damages incurred by these, nanobio-spectroscopy, Resonant Theranostics, aims to find narrow energy regions that correspond to *resonant or enhanced* absorption or emission (right fig)
- Spectroscopically targeted radiation - efficient with reduced exposure & provides detailed information

PRESENT: X-ray spectroscopy of the Br compound, bromodeoxyuridyne (BUdR), widely used as radiological contrast agent in radiation imaging

X-RAY SPECTROSCOPY OF Br

• Tumors could be radiosensitized by halogenated thymidine analogs, e.g. BUdR (fig), for breakup of DNA of tumor cells

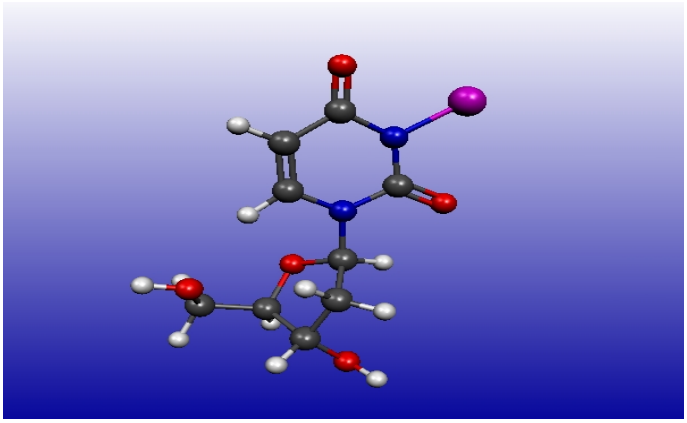

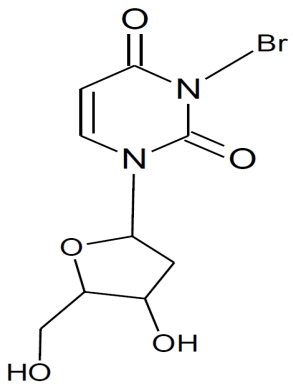

• The active element Br emits/ absorbs X-rays in narrow energy range: $\sim$ 12-14 keV (1s $\rightleftharpoons$ np)

• Heavy elements absorb/emit X-rays at higher energies where biogenic elements (H,C,N,O,CHON) are transparent

RESULTS: Oscillator strengths (f) for Auger K-shell 1s-np transitions, photoabsorption cross sections (σ), photon absorption coefficients ($\kappa = \sigma/m$)

We show i) κ **at resonant energies is much higher than the background and that of K-shell ionization**

ii) Resonant energy bands lie *below* **the K-shell ionization energy,** $I_K \sim 14$ **keV**

- **These are contrary to the aim of research focus at the K-shell ionization**

- **Targeting these energy bands, Auger processes can be initiated to produce larger number of photons and electrons via photon fluorescence and electron ejections.**

PHOTOABSORPTION: X(ion) + $h\nu \rightarrow X^+ + e$

X-RAY ABSORPTION BY Br AT K-SHELL EDGE

- **Figure shows *background photoinization* (resonances excluded) cross sections σ_{PI} of Bromine**
- **Rises in σ_{PI} correspond to enhancements in ionization at various K, L, M (sub)-shells energies**
- **Br K-shell ionization edge $\sim$ 14.0 keV. Enhanced ionization $\rightarrow$ ehnanced emission of electrons**

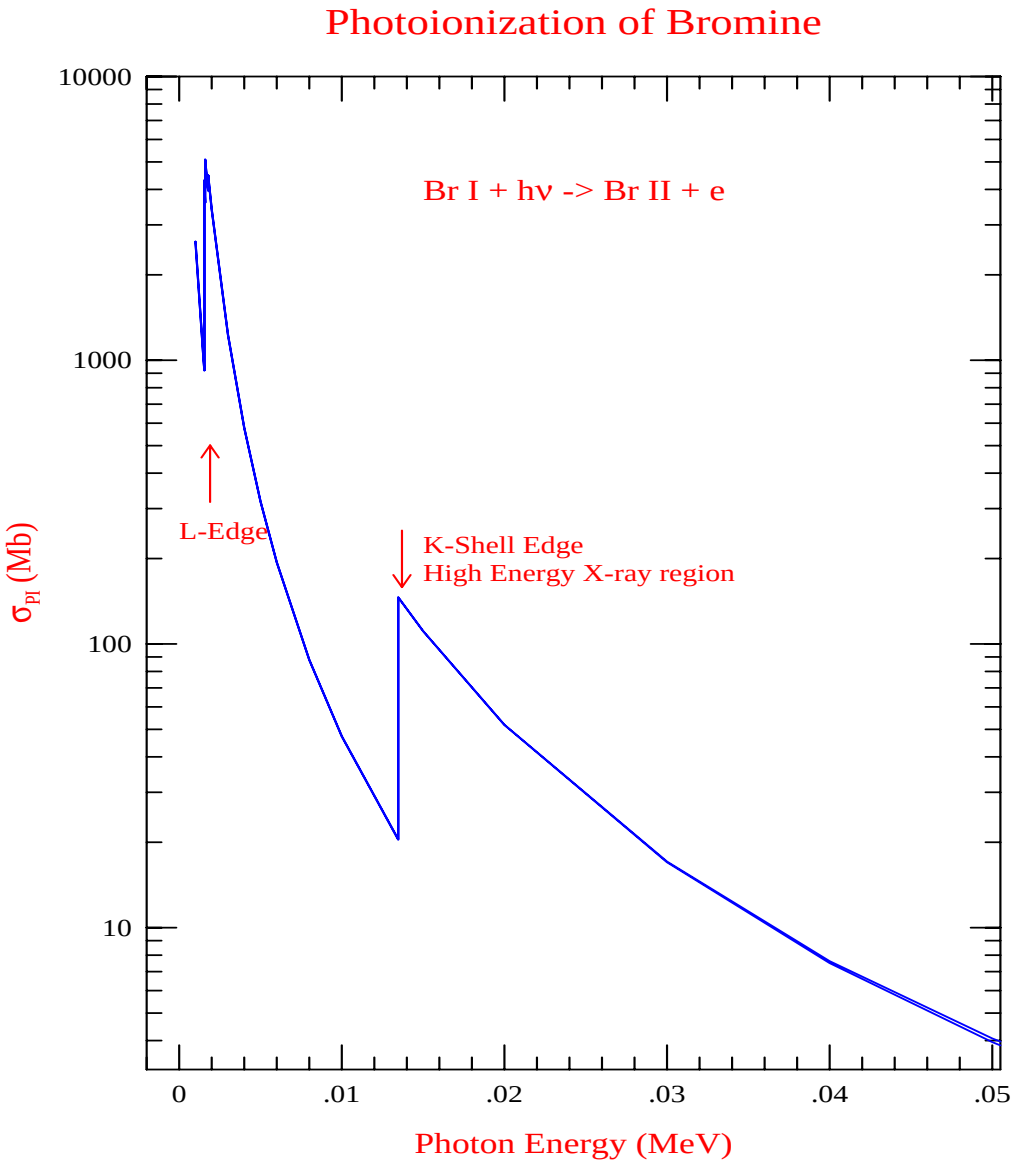

Auger Cascade: ELECTRON & PHOTON EMISSIONS

Auger Process: An electron from a higher level drops to fill a lower level vacancy, but emits a photon that can knock out another electron. This can lead to cascade as the vacancies move upward, more electrons and photons are emitted.

- **Fig (i) Ionization by X-ray photons (E_X) ($>$ K-shell ionization energy E_K) leading to Auger process**
- **Fig (ii) Multiple electron vacancies due to successive Auger decays leading to emission of photons and electrons**
- **Single ionization of 1s electron can lead to ejection of 20 or more electrons in an ion with occupied O and P shells**
- **Fig (iii) Inverse to Auger - Resonant photo-excitation from 1s $\rightarrow$ 2p (with L-shell vacancy) by an external monoenergetic X-ray source with intensity above our predicted critical flux**

$$\mathbf{\Phi^c(\nu_{K\alpha}) = \frac{\sum_{n_i \geq 2} g_i A[n_i(S_i L_i J_i) \rightarrow 2(SLJ)]}{g_K B_{K\alpha}}}. \qquad (1)$$

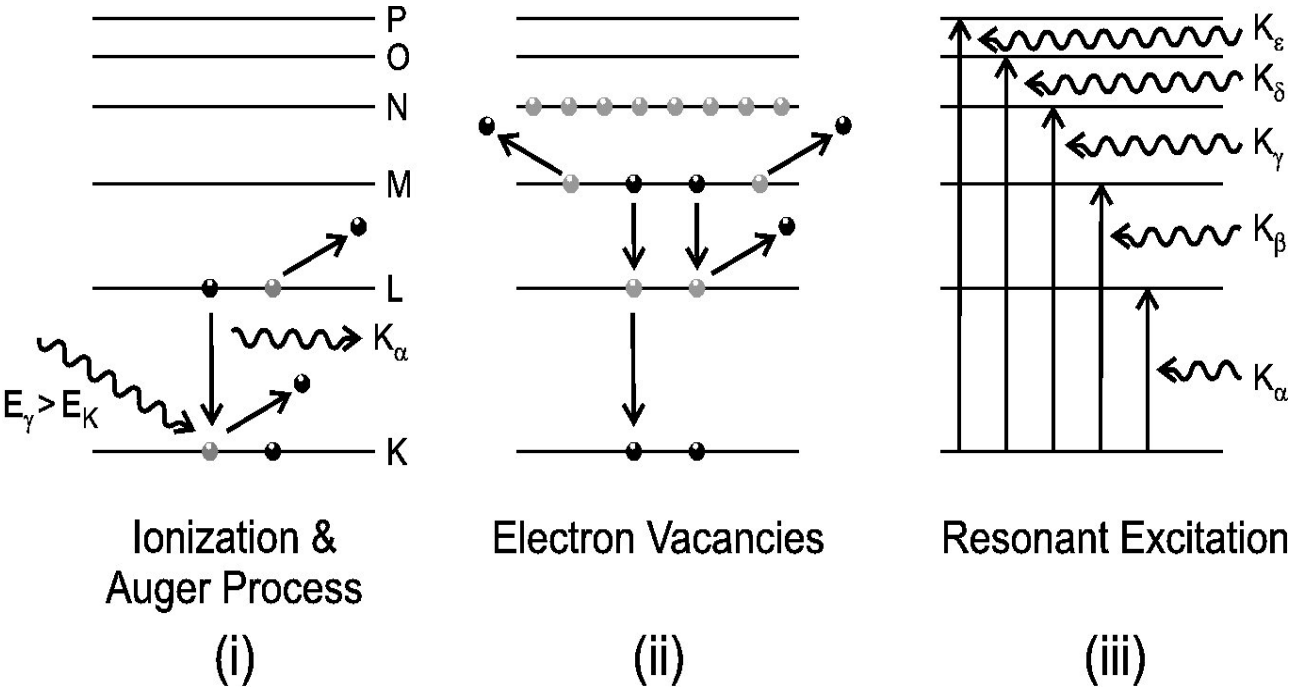

THEORY: RELATIVISTIC BREIT-PAULI APPROXIMATION

Relativistic effects: For a multi-electron system, the Breit-Pauli Hamiltonian is:

$$\mathbf{H_{BP} = H_{NR} + H_{mass} + H_{Dar} + H_{so} +}$$

$$\frac{1}{2}\sum_{i\neq j}^{N}[g_{ij}(so + so') + g_{ij}(ss') + g_{ij}(css') + g_{ij}(d) + g_{ij}(oo')] \qquad (2)$$

where the non-relativistic Hamiltonian is

$$H_{NR}\Psi = \left[\sum_{i=1}^{N}\left\{-\nabla_i^2 - \frac{2Z}{r_i} + \sum_{j>i}^{N}\frac{2}{r_{ij}}\right\}\right]\Psi = E\Psi \qquad (3)$$

one-body corrections terms are
$H_{mass} = -\frac{\alpha^2}{4}\sum_i p_i^4$, $H_{Dar} = \frac{\alpha^2}{4}\sum_i \nabla^2\left(\frac{Z}{r_i}\right)$, $H_{so} = \left[\frac{Ze^2\hbar^2}{2m^2c^2r^3}\right]$ **L.S the Breit interaction is**

$$H^B = \sum_{i>j}[g_{ij}(so + so') + g_{ij}(ss')] \qquad (4)$$

Wave functions and energies are obtained solving:

$$H\Psi = E\Psi$$

- $E < 0 \rightarrow$ **Bound (e+ion) states** Ψ_B
- $E \geq 0 \rightarrow$ **Continuum states** Ψ_F

Transition Matrix elements with dipole operator $D = \sum_i r_i$,

$< \Psi_B||D||\Psi_{B'} >$ $\rightarrow$ **Radiative Excitation and Deexcitation**
$< \Psi_B||D||\Psi_F >$ $\rightarrow$ **Photoionization and Recombination**

The matrix element reduces to generalized line strength,

$$\mathbf{S} = \left| \left\langle \Psi_\mathbf{f} | \sum_{\mathbf{j}=1}^{\mathbf{N+1}} \mathbf{r_j} | \Psi_\mathbf{i} \right\rangle \right|^2 \tag{5}$$

Oscillator Strength. Cross Section, Attenuation Coefficient

• The oscillator strength (f_{ij}) and radiative decay rate (A_{ji}) for the bound-bound transition are

$$\mathbf{f_{ij}} = \left[\frac{\mathbf{E_{ji}}}{\mathbf{3g_i}}\right] \mathbf{S}, \quad \mathbf{A_{ji}(sec^{-1})} = \left[\mathbf{0.8032 \times 10^{10}} \frac{\mathbf{E_{ji}^3}}{\mathbf{3g_j}}\right] \mathbf{S} \tag{6}$$

• The resonant structures of $K\alpha, K\beta, K\gamma, K\delta, K\eta$ complexes in photoionization cross sections σ_{PI} are obtained from Auger line strengths. For this, the resonant cross sections were convolved over a normalized gaussian function

$$\sigma_{\mathbf{K}\alpha}(\nu; \mathbf{K} \rightarrow \mathbf{L_i}) = \frac{\mathbf{4\pi^2 a_o^2 \alpha}}{\mathbf{3}} \frac{\mathbf{E(K - L_i)}}{\mathbf{g_k}} \mathbf{S(K - L_i)} \phi(\nu) = \mathbf{4\pi^2 a_o^2 \alpha f_{KL_i}} \phi(\nu) \tag{7}$$

where $\phi(\nu)$ the Gaussian profile with width ΔE,

$$\phi(\nu) = \frac{\mathbf{1}}{\sqrt{\mathbf{2\pi}}\mathbf{\Delta E}} \exp\left(-\frac{\mathbf{E^2}}{\mathbf{2\ \Delta E^2}}\right)$$

• The mass attenuation coefficient per volume mass, κ is

$$\kappa_{\text{res}}(\nu; \mathbf{K}\alpha) = \frac{\sigma_{\mathbf{tot}}}{\rho} = \frac{\mathbf{1}}{\mathbf{uW_A}} \frac{\sum_\mathbf{j} \mathbf{w_j} \sigma_{\text{res}}(\nu; \mathbf{K - L_{ji}})}{\sum_\mathbf{j} \mathbf{w_j}} \tag{8}$$

where u is 1 amu, W_A = atomic weight, w_j=statistical weight

RESONANT $K_{\alpha,\beta}$ (1s-np) TRANSITIONS IN Br

- The table presents data for resonant $K-$shell $(1s-np)$ transitions in
Br II ($1s^2 2s^2 2p^6 3s^2 3p^6 3d^{10} 4s^2 4p^4$)
- Auger transitions are initiated with K-shell ionization of Br I
- Table values are the averaged resonant energy, $E(K_{\alpha,\beta,\gamma})$, and the corresponding oscillator strength f and photoionization cross section, σ_{res})
- Each transition corresponds to a large number of fine structure transitions
- These resonance strengths provide the dominant contribution to photo-absorption, far more than K-shell ionization

Transition Array	# of Transitions	$E(K_\alpha)$ (keV)	f_{tot}	$\langle\sigma_{res}(K_\alpha)\rangle$ (Mb)
$1s2s^22p^5...4p^5$ -$1s^22s^22p^5...4p^4$	30	8.809E+02	1.03E+00	8.31E+00
$1s2s^22p^5...4p^5$ -..$3s^23p^5...4p^4$	30	9.864E+02	8.00E-02	6.45E-01
$1s2s^22p^6...4p^5$ -$4p^44f$	59	9.993E+02	7.12E-09	5.74E-08
$1s2s^22p^6...4p^5$ -..$4s^24p^5$	14	1.001E+03	1.34E-04	1.08E-03

X-ray Absorption Spectrum of Bromine

- **Figure: X-ray mass photo-absorption coefficient $\kappa(cm^2/g)$**
- **The resonances, due to K $\rightarrow$ L, M, N transitions, lie between E = 12 - 13.6 keV, below the K-edge**
- **Photo-absroption by the K-complex resonances exceed the background by more than an order**
- **Note, not studied before, that K-complex resonances are higher than the jump at K-shell ionization**

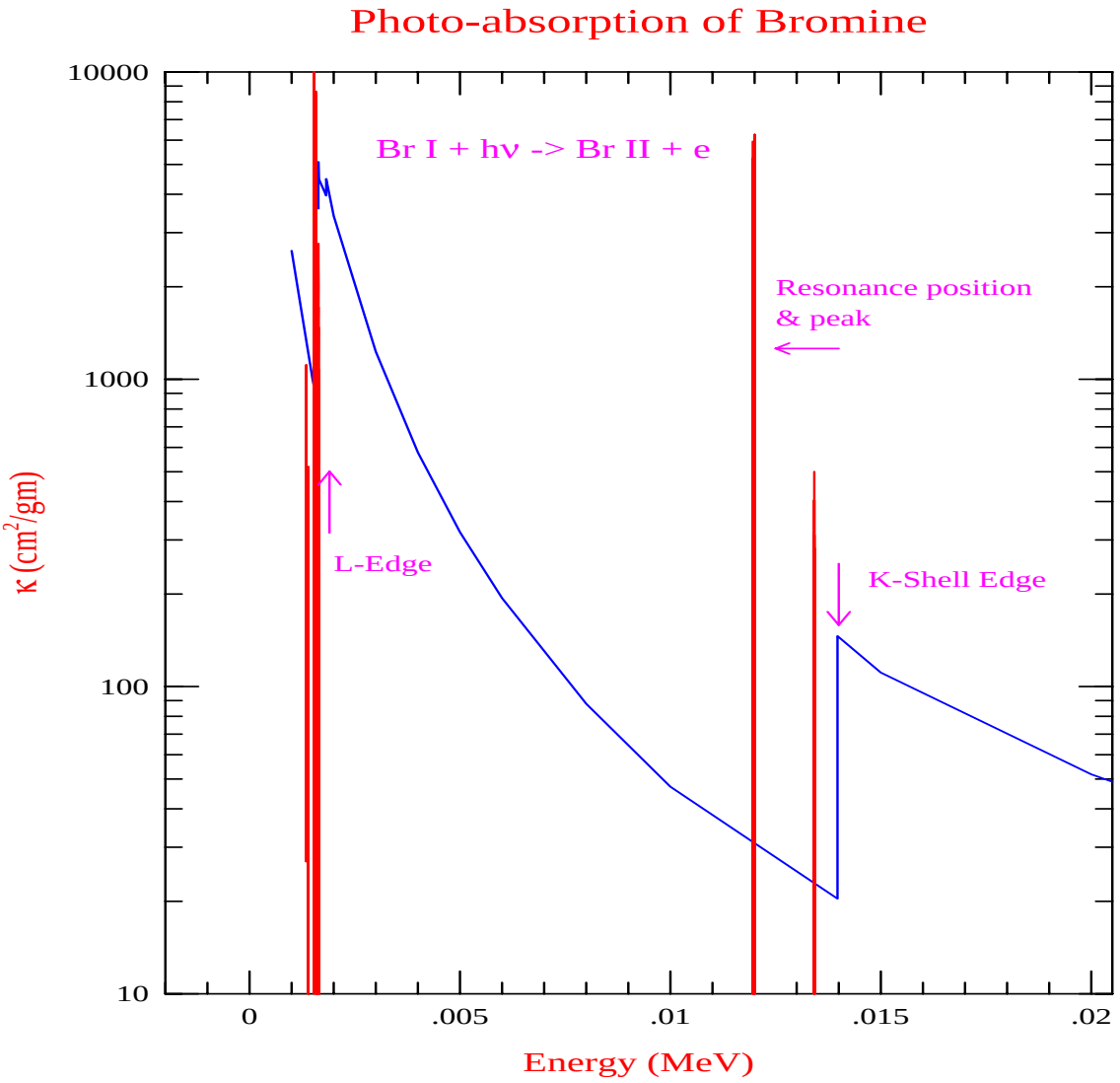

Monte Carlo Simulation for Resonant K_α X-Ray Absorption by Au Nanoparticles

(Montenegro et al. 2009)

- **TOP:** Geomtry of the experiment - the phantom (15 x 5 x 5 cm) models a tumor embedded with gold nanoparticles (golden section 2 cm) 10 cm inside normal tissue (blue section)
- **BOTTOM:** Simulation - gold nanoparticles at 5 mg/ml, X-ray beam at resonant energy $\sim$ 68 keV
- **NOTE:** Because of Compton scattering only a few photons reach the region with gold nanoparticles

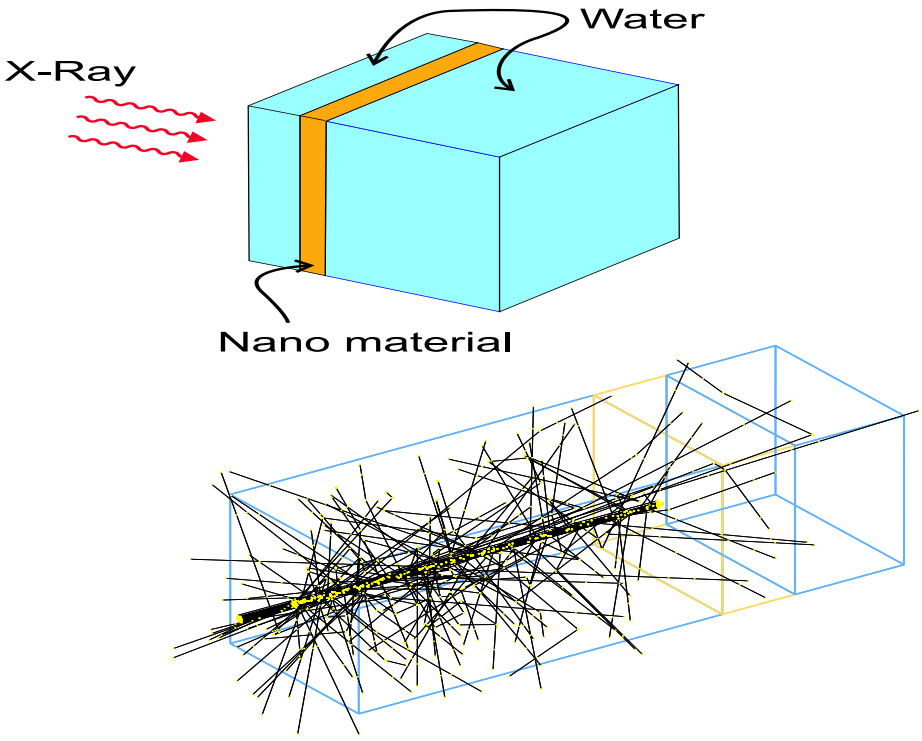

X-RAY ABSORPTION BY Au AT 68 keV, 82 keV, 2 MeV

Figure: X-ray energy deposited by depth in the phantom: Red curve - with tumor in region 100 to 120 mm embedded with gold nanoparticles at 5 mg/ml, Blue curve - only water

- **Top:** X-ray at 68 keV - averaged Kα resonant energy
- **Middle:** 82 keV - just above K-edge ionization energy
- **Bottom:** 2 MeV - high energy common in clinical usage
- The presence of gold nanoparticles has increased the energy deposited at the tumor
- The highest absorption, by more than 25 time that at 82 keV, is at the resonant energy 68 keV (top panel)

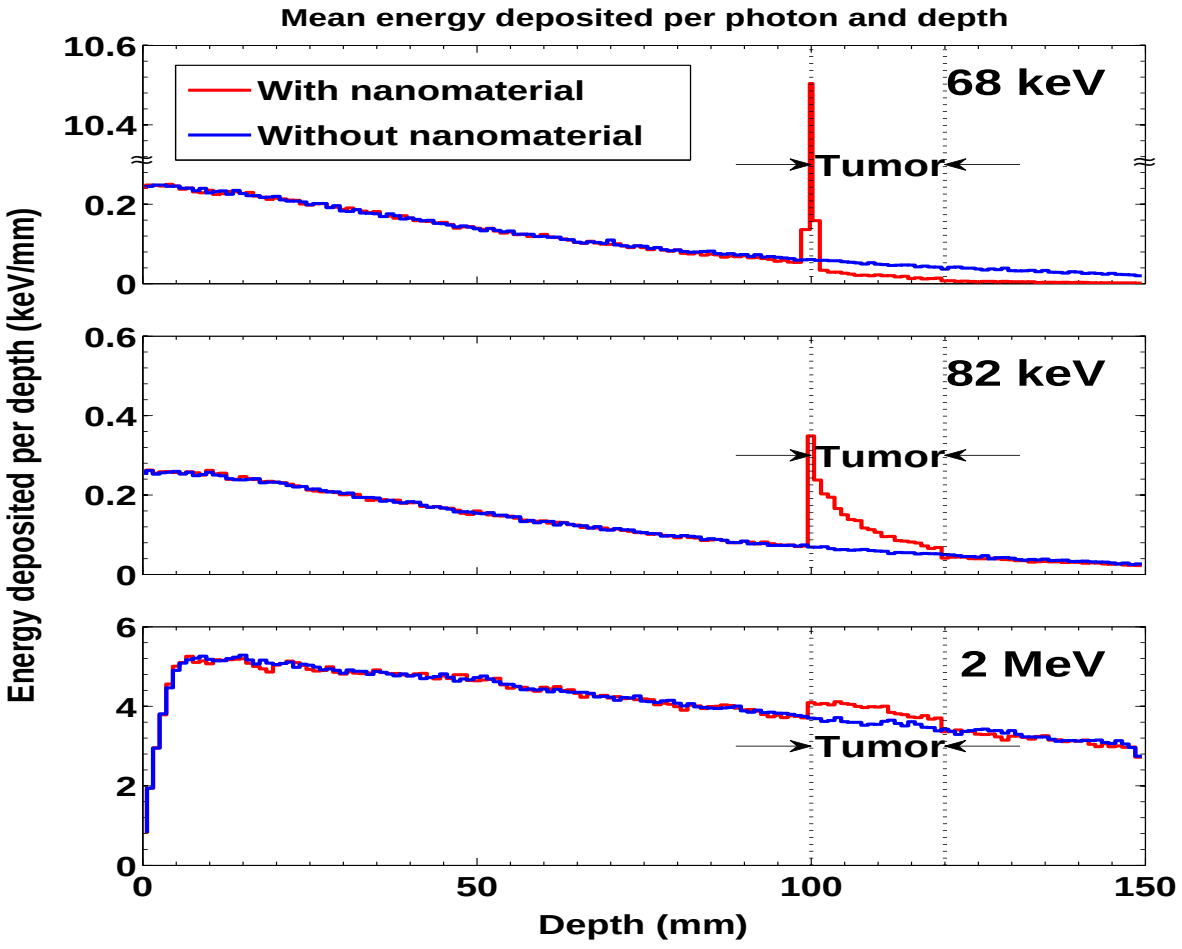

ELECTRON PRODUCTIONS AT 68 keV, 82 keV, 2 MeV

Figure: Number of Auger electrons produced with depth following X-ray absorptions: Red curve - tumor embedded with gold nanoparticles at 5 mg/ml in region 100 to 120 mm, Blue curve - only water

- **Top:** X-ray at 68 keV - averaged Kα resonant energy
- **Middle:** 82 keV - just above K-edge ionization energy
- **Bottom:** 2 MeV - high energy common in clinical usage
- A considerably large number of electrons, by more than an order of mangitude, were produced by 68 keV X-rays compared to those by 82 keV and 2 MeV

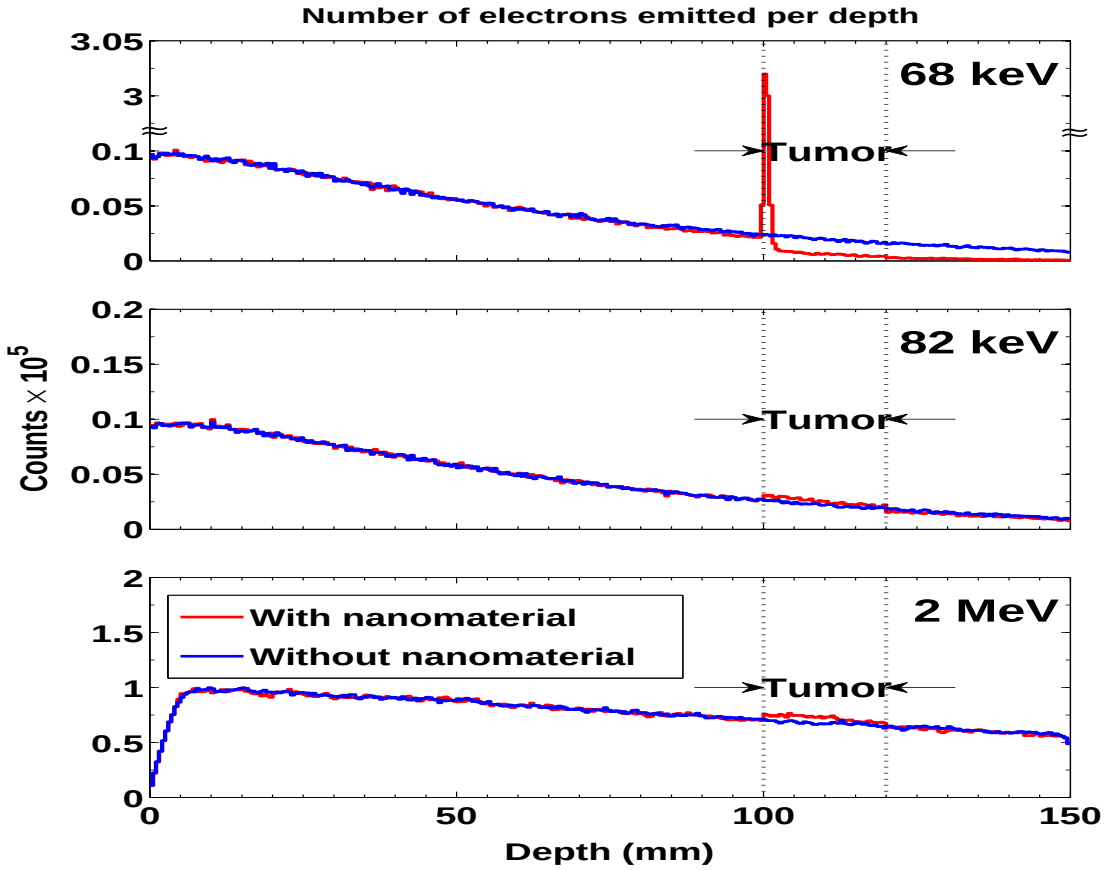

CONCLUSION

1. **We present X-ray spectroscopy of the Br in BUrD where we predict resonant energies below the K-shell ionization threshold for enhanced X-ray absorption**
2. **We obtained Auger resonant probabilities and cross sections to obtain total mass attenuation coefficients with resonant cross sections**
3. **We find that the attenuation coefficients for X-ray absorptions at resonant energies are much larger, over an order of magnitude, higher over the background cross section as well as to that at K-edge threshold**
4. **The simulation for gold predicts enhanced X-ray absorption and follow-up enhanced electron and photon emissions at resonant energies.**